SPECIAL
Climate and Frontal Air-Sea Interaction
COLLECTION

The Annual Cycle of the Japan Sea Throughflow

SHINICHIRO KIDA

Application Laboratory, Japan Agency for Marine-Earth Science and Technology, Yokohama, Japan

BO QIU

Department of Oceanography, University of Hawaiʻi at Mānoa, Honolulu, Hawaii

JIAYAN YANG

Department of Physical Oceanography, and OUC-WHOI Joint Research Center, Woods Hole Oceanographic Institution, Woods Hole, Massachusetts

XIAOPEI LIN

Physical Oceanography Laboratory, and OUC-WHOI Joint Research Center, Ocean University of China, and Qingdao Collaborative Innovation Center of Marine Science and Technology, and Function Laboratory for Ocean Dynamics and Climate, Qingdao National Laboratory for Marine Science and Technology, Qingdao, China

(Manuscript received 14 April 2015, in final form 22 September 2015)

ABSTRACT

The mechanism responsible for the annual cycle of the flow through the straits of the Japan Sea is investigated using a two-layer model. Observations show maximum throughflow from summer to fall and minimum in winter, occurring synchronously at the three major straits: Tsushima, Tsugaru, and Soya Straits. This study finds the subpolar winds located to the north of Japan as the leading forcing agent, which first affects the Soya Strait rather than the Tsushima or Tsugaru Straits. The subpolar winds generate baroclinic Kelvin waves along the coastlines of the subpolar gyre, affect the sea surface height at the Soya Strait, and modify the flow through the strait. This causes barotropic adjustment to occur inside the Japan Sea and thus affect the flow at the Tsugaru and Tsushima Straits almost synchronously. The barotropic adjustment mechanism explains well why the observations show a similar annual cycle at the three straits. The annual cycle at the Tsugaru Strait is further shown to be weaker than that in the other two straits based on frictional balance around islands, that is, frictional stresses exerted around an island integrate to zero. In the Tsugaru Strait, the flows induced by the frictional integrals around the northern (Hokkaido) and southern (Honshu) islands are in opposite directions and tend to cancel out. Frictional balance also suggests that the annual cycle at the Tsugaru Strait is likely in phase with that at the Soya Strait because the length scale of the northern island is much shorter than that of the southern island.

1. The Japan Sea and the North Pacific

The Japan Sea is a marginal sea located in the western North Pacific. It is deep (about 1500 m) but semienclosed from the North Pacific by the Japanese Archipelago. What makes this sea unique among the various marginal seas located in the western North Pacific is that the four straits that connect the Japan Sea to its surrounding seas, the Tsushima, Tsugaru, Soya, and Tartar Straits (Fig. 1), are only 150 m deep or shallower. The Japan Sea is therefore influenced by the in/outflows through these straits near the surface, while the deeper part of the basin is separated from other seas. Observations show that about 2–3 Sverdrups (Sv; $1\,\mathrm{Sv} \equiv 10^6\,\mathrm{m^3\,s^{-1}}$) of water mass exchange occurs across the straits on annual average [see Talley et al. (2006) and reference therein]. Although this transport magnitude is significantly less than that of the

Corresponding author address: Shinichiro Kida, Application Laboratory, Japan Agency for Marine-Earth Science and Technology, 3173-25 Showa-machi, Kanazawa-ku, Yokohama 236-0001, Japan.
E-mail: kidas@jamstec.go.jp

DOI: 10.1175/JPO-D-15-0075.1

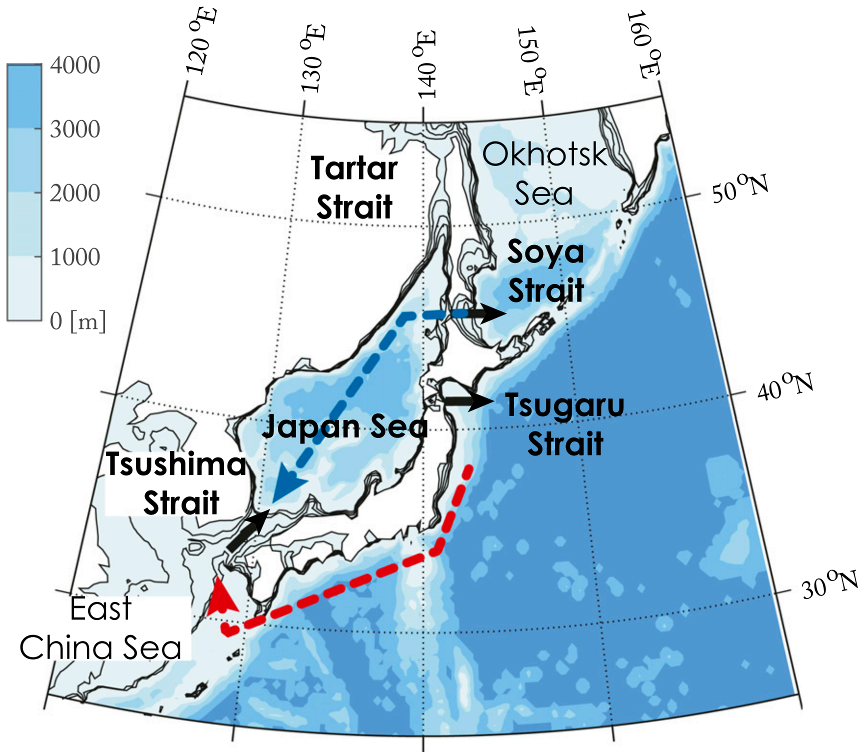

FIG. 1. The topography and straits of the Japan Sea. The black solid arrows show the direction of the annual-mean Throughflow at the straits. The dashed arrows indicate the pathways of the waves that enter the Tsushima Strait from the subpolar region (blue) and the subtropical region (red).

Kuroshio (about 40–50 Sv along the southern coast of Japan; e.g., Imawaki et al. 2001), the exchange flows play a critical role in determining the upper oceanic circulation and sea surface temperature (SST) in the Japan Sea. Recent studies show that the SST variability affects not only the local atmospheric conditions (Hirose and Fukudome 2006) but also the East Asian monsoonal climate (Yamamoto and Hirose 2011; Seo et al. 2014).

The upper oceanic circulation in the Japan Sea consists of an inflow from the south (Tsushima Strait) and outflows to the northeast (Tsugaru and Soya Straits). The inflow is known as the Tsushima Warm Current, and its annual-mean transport, according to long-term measurements from bottom-mounted ADCP (Teague et al. 2002) and ship-mounted ADCP (Isobe et al. 2002; Takikawa et al. 2005), is about 2.4–2.7 Sv. The Tsushima Warm Current bifurcates to a flow along the coast of Japan and a flow along the Korean Peninsula, which then crosses the Japan Sea zonally at about 40°N (Talley et al. 2006). The outflows are known as the Tsugaru trait Warm Current and Soya Strait Warm Current. Geostrophic transport estimates from hydrography suggest the annual-mean transport of the Tsugaru Strait Warm Current to be about 1.5 Sv (Onishi and Ohtani 1997), which is supported by ADCP measurements (Shikama 1994; Nishida et al. 2003). Observations at the Soya Strait have been limited, but recent year-long bottom-mounted ADCP measurements reveal an annual-mean transport of about 1.0 Sv (Fukamachi et al. 2008). The flow through the Tartar Strait is considered negligible because of its narrow width (about 7 km) and shallow depth (about 4 m) (Fukamachi et al. 2008). We will refer to this system of flows that occur across the straits as the Japan Sea Throughflow or simply Throughflow hereinafter (Fig. 1).

a. The observed annual cycle

The basic mechanism responsible for driving the annual-mean transport of the Throughflow has been intensively studied (e.g., Minato and Kimura 1980; Ohshima 1994; Tsujino et al. 2008) and most of these studies suggest the annual-mean wind stress over the North Pacific to be responsible. However, the mechanism responsible for driving the annual cycle of the Throughflow transport remained an open question partly because observations have been insufficient to describe seasonal changes at all three straits, especially at the Soya Strait (Fukamachi et al. 2008). Among the three straits, the Tsushima Strait is the most frequently observed [see Teague et al. (2006) and reference therein]. Past direct measurements reveal an annual cycle at the Tsushima Strait with a maximum

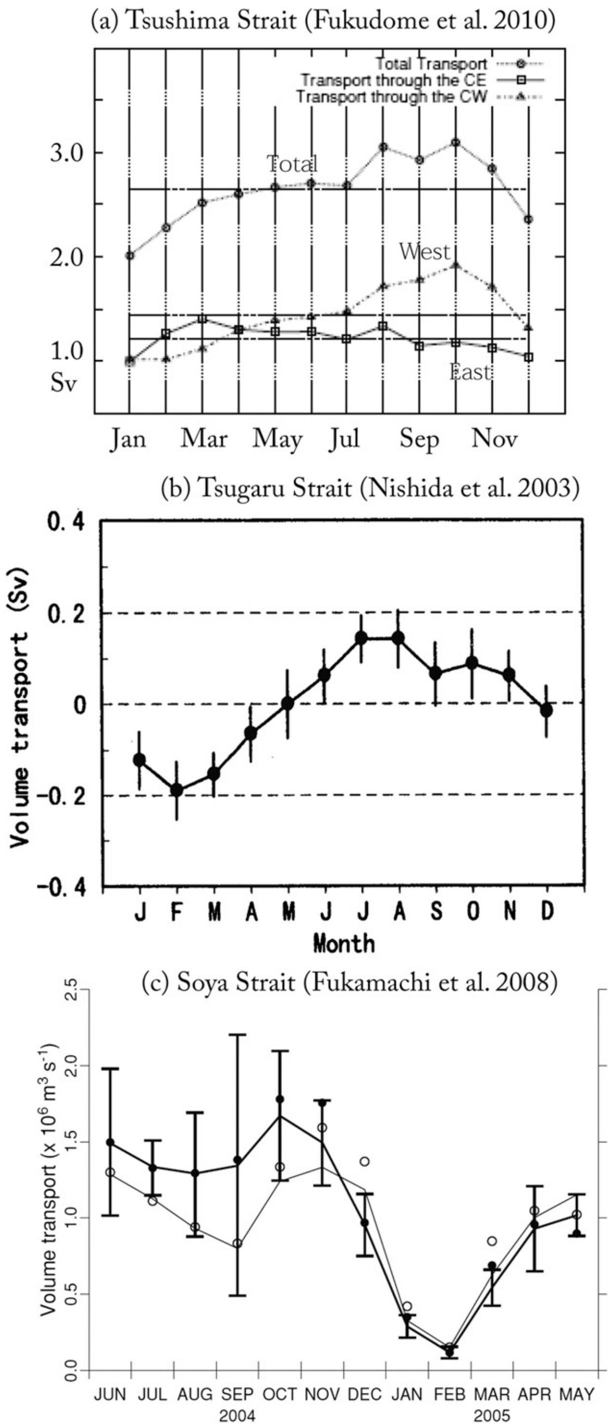

FIG. 2. The annual cycle of the transport observed at the (a) Tsushima (Fig. 6 of Fukudome et al. 2010), (b) Tsugaru (Fig. 12 of Nishida et al. 2003), and (c) Soya (Fig. 5a of Fukamachi et al. 2008) Straits. Note that (b) is anomaly, and (c) is not the climatology and starts from June.

transport from late summer to early fall and a minimum transport in winter (Fig. 2a; Fukudome et al. 2010). The amplitude of seasonal cycle in transport is about 0.8–1.7 Sv (Isobe et al. 2002; Teague et al. 2002; Takikawa et al. 2005), and the transport in the western half of the strait appears to show a more robust annual cycle (Fukudome et al. 2010). Long-term estimates based on the sea level differences across the Tsushima Strait indicate a similar annual cycle (Lyu and Kim 2003; Takikawa and Yoon 2005), although these estimates may contain errors from baroclinic effects (Lyu and Kim 2003). Observations at the Tsugaru and Soya Straits, on the other hand, are much limited but nevertheless show a similar annual cycle in transport with a magnitude of about 0.4 (Fig. 2b; Nishida et al. 2003) and 1.5 Sv (Fig. 2c; Fukamachi et al. 2008), respectively. Past observational studies therefore indicate that the leading balance of the annual cycle in volume transport through the Japan Sea is mainly between those crossing the Tsushima and Soya Straits. This is different from the annual mean, where the leading balance is mainly between those crossing the Tsushima and Tsugaru Straits. The significance of the Soya Strait on the annual cycle is quite surprising considering that this strait is only 40 m deep, less than half of that at the Tsugaru Strait (140 m). On the other hand, the Soya Strait is about 40 km wide, which is twice the width of the Tsugaru Strait (20 km). The Tsushima Strait is about 150 m deep and 150 km wide, deeper and wider than either of the two outflow straits.

There are two notable aspects about the annual cycle observed at the three straits (Figs. 2a–c). First, the annual cycle occurs roughly in phase at all straits with the smallest signal observed at the Tsugaru Strait. Second, the phase of the annual cycle of the Throughflow is opposite to what would be expected for a western boundary current (WBC) of a flat-bottom ocean, driven by the annual cycle of the wind stress curl in the interior of the subtropical North Pacific. The strongest wind stress curl is observed in winter so the maximum Throughflow would be expected to occur in winter, assuming a Sverdrup-balanced wind-driven gyre. Barotropic Rossby waves could travel across the Pacific basin and induce an annual cycle in the WBC in a few days, which would then increase the pressure gradient between the straits and drive a stronger Throughflow. Observations show the Throughflow changing in the opposite phase and therefore suggest that some other processes are at work affecting or driving the annual cycle of the Throughflow.

b. The mechanism driving the annual cycle

How is the annual cycle of the Throughflow induced at the straits? Based on the two aspects mentioned above, specific questions are as follows:

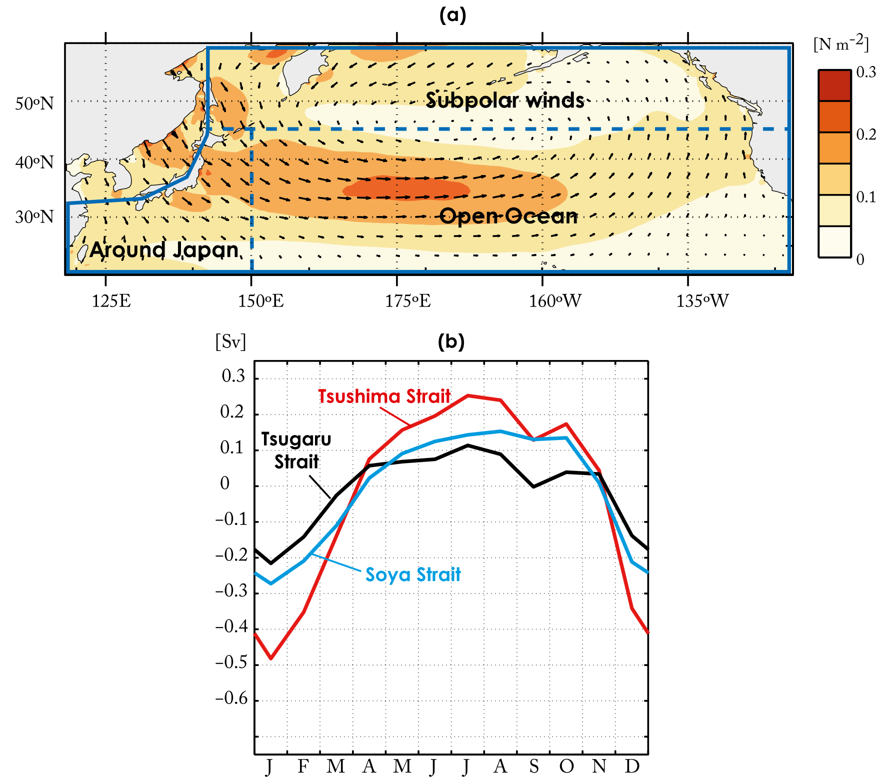

FIG. 3. (a) The model domain of the two-layer model (RTOPO) with wind stress in January. Colors indicate the magnitude, and the vectors show their direction. The solid box shows the forcing region for the winds outside the Japan Sea. Dashed lines show the forcing regions for experiments with only subpolar winds, subtropical winds around Japan, or subtropical winds in the open ocean. (b) The annual cycle of the Throughflow at the Tsushima (red), Tsugaru (black), and Soya (blue) Straits.

1) What is the primary forcing agent and why is the phase of the annual cycle similar at all of the three straits?
2) Why is the annual cycle at the Tsugaru Strait weaker than that in the other two straits?

We will answer these questions beginning by discussing the annual cycle of the Throughflow at the Tsushima Strait. This is because the flow through this strait is by far the best observed and investigated.

The annual cycle of the Throughflow at the Tsushima Strait is likely induced by the seasonally varying winds. The magnitude of the winds from spring to fall is much weaker compared to that in winter, when the East Asian Monsoon results in strong northwesterly winds over the Japan and Okhotsk Seas and westerly and easterly winds in the subtropical and subpolar open ocean, respectively (Fig. 3a). The local winds over the Tsushima Strait can force surface Ekman transport with a similar phase as that of the Throughflow. However, this local forcing mechanism appears insufficient since its magnitude is only about 0.1 Sv (Fukudome et al. 2010), which is an order of magnitude smaller than that observed (Figs. 2a–c). Nevertheless, Moon et al. (2009) show that the along-strait wind over the Tsushima Strait in September, which is related to tropical cyclones, is responsible for the drop in the Throughflow in September. While the role of local winds may become important for part of the year, it appears insufficient in explaining the whole annual cycle, which suggests that processes that are likely of remote origins induce the majority of the annual cycle of the Throughflow.

By using a numerical model, Cho et al. (2013) suggest the importance of the winds over the East China Sea for explaining the maximum transport through the Tsushima Strait in fall. These winds drive the onshore transport across the shelf break of the East China Sea. While this mechanism matches with the intrusion of Kuroshio to the Tsushima Strait in fall in terms of mass balance (Guo et al. 2006; Isobe 2008), the dynamics that connects the onshore flow and the Tsushima Current is unclear. Topographic waves from the shelf break in the East China Sea should propagate southward (Andres et al. 2011). This would make the Tsushima Strait upstream, not downstream, to forcing that occurs in the East China Sea. How such annual signals from the East China Sea can propagate to the strait is not clear in terms of dynamics. The annual cycle of the onshore transport is also at a minimum in July and a maximum in October and cannot explain the transport minimum in winter. The winds over the East China Sea appear implausible in explaining the whole annual cycle of the Throughflow.

Several other hypotheses have been proposed as the remote forcing mechanisms, and they can be roughly categorized into two, with the differences arising from the possible pathways of waves entering the Tsushima Strait. The first hypothesis considers the seasonal signal at the Tsushima Strait to enter from the south along the east coast of Japan (Fig. 1). Ma et al. (2012) suggest the annual cycle of the Kuroshio along the coast of Japan, which is driven by the open oceanic winds, as the forcing agent. When the Kuroshio transport increases, it enhances the frictional drag and the pressure gradient along the east coast of Japan. The pressure difference will be felt on the west coast of Japan, which would increase the Throughflow transport. The mechanism responsible for the annual cycle of the Throughflow at the Tsugaru and Soya Straits, however, remain unexplained. The mechanism may also depend on the details of the Kuroshio near the coast. Observations of the total integrated Kuroshio transport south of Japan show the minimum in fall and maxima in winter and early summer (Isobe and Imawaki 2002), which does not correlate well with the Tsushima Current. By using the time series of the Tsushima Current transport based on submarine cable and sea level height at tidal stations around Japan and Korea, Lyu and Kim (2005) suggest the importance of the sea level changes induced on the Pacific side of the Tsushima Strait for the seasonal to interannual time scales. How this sea level change is related to various forcing and to transports through the Soya Strait is still uncertain. Seung et al. (2012) then made an effort to discuss the annual cycle at all three straits. They suggested the winds to the east of Japan as the primary forcing agent by extending the island rule (Godfrey 1989) with that incorporating bottom friction at the straits (Seung 2003). The oceanic winds drive the WBCs along the east coast of Japan, which would create a pressure gradient across the three straits. The annual cycle of the Throughflow at the Tsugaru Strait is shown to be small because the impact from the subpolar and subtropical winds cancels out at its latitude. This hypothesis suggests that the flows through the Tsushima and Soya Straits are not dynamically connected and are in phase because the open oceanic winds are in phase. The shortcoming of this mechanism is that the original island rule is based on a flat-bottom ocean and a steady-state assumption and thus is inappropriate for application to the annual cycle with shallow straits. Topography has large influence on the dynamics behind the island rule (Yang et al. 2013). So it remains unexplained how the annual cycle of the open oceanic winds drives the Throughflow. Even if the topography is flat everywhere, the annual cycle of the winds' stress curl in the open ocean to the east of Japan suggests maximum transport at the Tsushima strait from fall to winter and minimum in summer, as mentioned earlier, opposite to what is observed. Moreover, the magnitude of the Throughflow would then be on the order of the wind-driven gyre, which is an order larger.

The second scenario considers the seasonal signal at the Tsushima Strait to enter from the north (Fig. 1). Tsujino et al. (2008) first suggested this mechanism and hypothesized that the seasonal signal is induced at the Soya Strait, which then propagates across the Japan Sea as an internal Kelvin wave and reaches the Tsushima Strait. The annual cycle of the subpolar winds, especially that over the Okhotsk Sea, is the primary forcing agent for inducing the annual cycle at the Soya Strait. This mechanism successfully explains why the Throughflow transports at the Soya and Tsushima Straits vary annually with similar magnitude and in phase. It is also consistent with the findings of Cho et al. (2009), who utilized a GCM and found the annual cycle of the Throughflow transport at the Tsushima Strait to correlate better with that at the Soya Strait than the Tsugaru Strait. However, the validity of this second scenario remains unclear because the presence of seasonal internal coastal Kelvin waves, which is essential for propagating the seasonal signal from the Soya Strait to the Tsushima Strait, has not been found yet observationally. The mechanism also assumes that the waves propagating along the east coast of Japan dissipate sufficiently and do not reach the Tsushima Strait. While the presence of the Kuroshio along the coast of Japan may be partly responsible for the enhanced dissipation, how well this assumption holds is unclear.

c. *Our hypothesis*

In this manuscript, we hypothesize that the subpolar wind stress is the primary forcing agent of the annual cycle of the Throughflow, similar to the second hypothesis put forth above. The winds north of the Soya Strait are suggested to play a central role, especially those along the coastlines. We will further suggest that barotropic adjustment in the Japan Sea is what connects the annual cycle at the three straits, not the internal Kelvin waves as suggested by Tsujino et al. (2008). While more details about this mechanism will be explained later, our hypothesis is motivated by the sensitivity experiments from a two-layer model of the North Pacific and the Japan Sea.

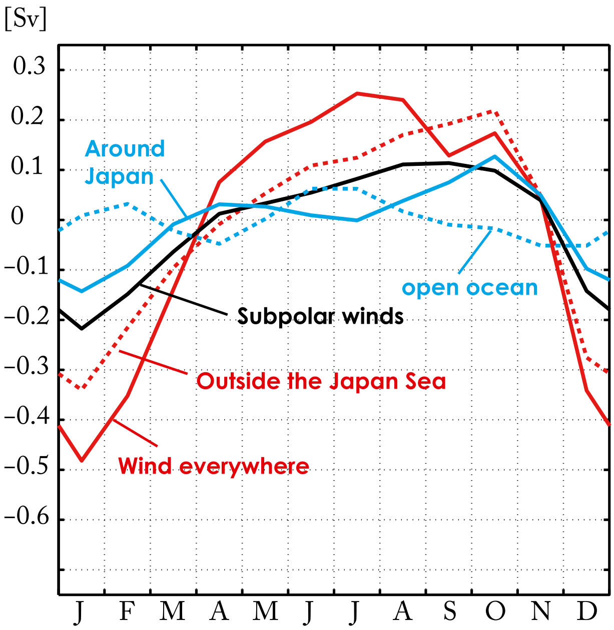

FIG. 4. The annual cycle of the transport simulated at the Tsushima Strait when forced by winds over the whole model domain (solid red, as in Fig. 3b), winds outside the Japan Sea (dashed red), subpolar winds (solid black), subtropical winds around Japan (solid blue), and subtropical winds in the open ocean (dashed blue). See Fig. 3a for where the winds are forced.

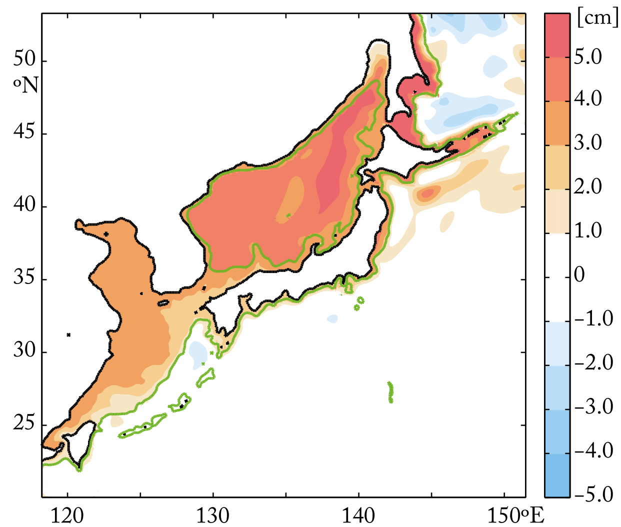

FIG. 5. The monthly mean SSH of January from RTOPO that is forced only by the subpolar winds. The majority of the SSH signals in the Japan Sea occur uniformly.

When a two-layer model with realistic topography of the North Pacific and the Japan Sea is forced by the seasonally varying climatological ERA-Interim wind stress (monthly means minus annual mean; Dee et al. 2011), it simulates the annual cycle that is analogous to that observed (Fig. 3). Maximum transport occurs in summer and minimum transport occurs in winter (Fig. 3b). The bottom topography is based on the 1-minute gridded elevations/bathymetry for the world (ETOPO1) with a minimum depth of 10 m, and the horizontal resolution is 1/12 of a degree, capable of resolving the straits. The effect of sea ice is not included, but models with no ice are shown capable of capturing the basic flow field in the Okhotsk Sea (Ohshima and Simizu 2008; Nakanowatari and Ohshima 2014). We will refer to the experiments based on the setup as RTOPO hereinafter. What RTOPO show is that the basic annual cycle can be simulated by the winds outside the Japan Sea (Fig. 4). Among the winds outside the Japan Sea, the subpolar winds are playing the leading role. The role of subtropical winds around Japan is secondary for most of the months, and the role of subtropical winds in the open ocean is negligible. Modeled maximum transport in summer rather than toward the fall is likely a result of stronger ERA-Interim wind stress over the Tsushima Strait compared to observations. Surface Ekman transport with an annual cycle of about 0.25 Sv and a maximum in July is driven in the model, which is twice that observed (~0.1 Sv; Fukudome et al. 2010). The numerical experiments support the hypothesis that the annual cycle of the Throughflow is forced remotely and moreover that the subpolar winds act as the leading forcing agent. RTOPO also show that the majority of the sea surface height (SSH) variability in the Japan Sea occurs uniformly rather than via waves trapped along the coastline (Fig. 5). The SSH in the Okhotsk Sea, on the other hand, shows a coastally trapped signal, as discussed in Nakanowatari and Ohshima (2014). The spatial uniformity of the SSH variability in the Japan Sea suggests that this sea is responding barotropically rather than baroclinically. Such a barotropic response of the Japan Sea has been suggested to occur in the nonseasonal band (Kim and Fukumori 2008), and our experiments here suggest that a similar process may occur for the annual cycle as well.

In order to understand the processes responsible for driving the annual cycle of the Throughflow in RTOPO better, we will utilize a two-layer model with an idealized topographic setting. This is to isolate the basic topographic features, which affect how the waves propagate between the open ocean and the marginal sea through the modification of the background potential vorticity (PV) field (Yang et al. 2013). We will also focus on the role of the subpolar winds. Details of this idealized model will be described next in section 2, and the results are presented in section 3. The role of barotropic waves and continental slopes are discussed. We will then examine the dynamics responsible for the annual cycle at the Tsugaru Strait in section 4. A summary and final remarks are given in section 5.

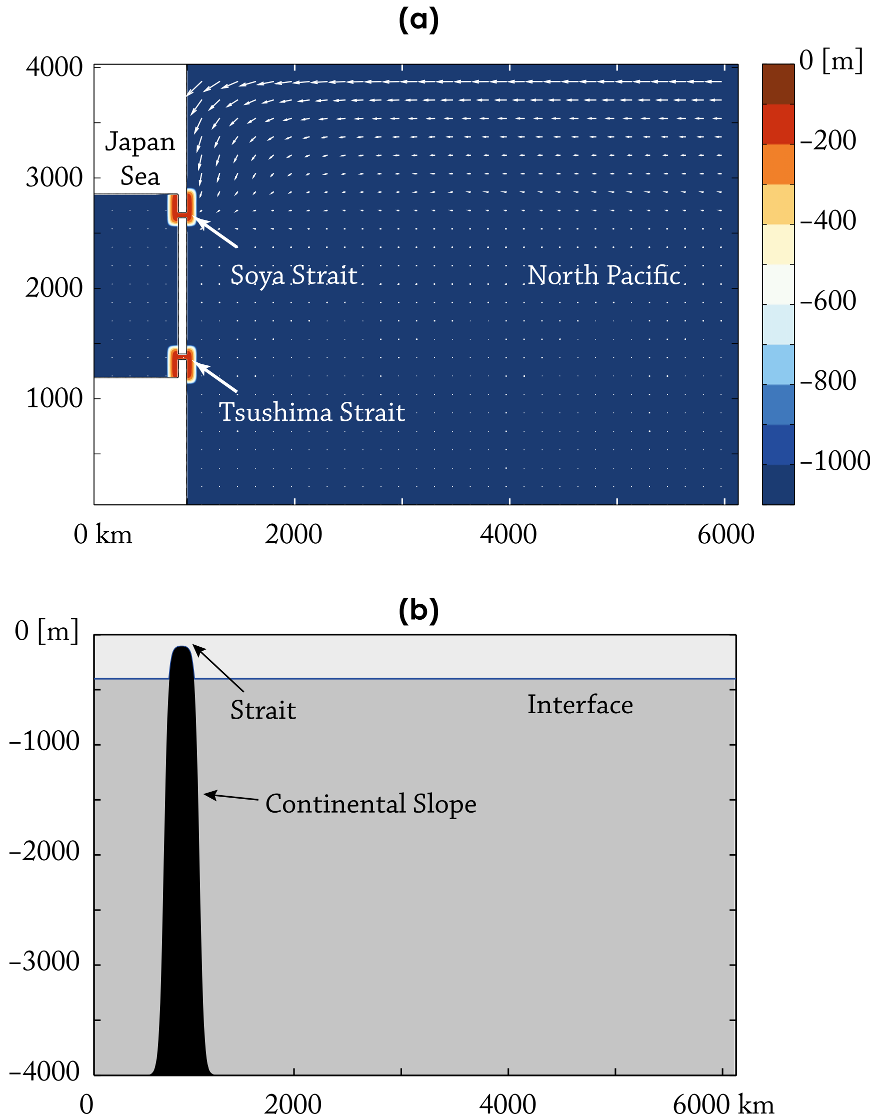

FIG. 6. (a) The model domain and bottom topography in CTRL. The straits that connect the Japan Sea and the North Pacific are both 40 km wide and 100 m deep. White vectors show the wind stress pattern in January. (b) Zonal cross section at the latitude of the straits. The strait is located at the top of the steep continental slope. The interface lies at 400-m depth.

2. Model setup

a. The control experiment

A two-layer model based on Hallberg isopycnal model (HIM) is used (Fig. 3; Hallberg 1997). The momentum and thickness equations are

$$\frac{\partial \mathbf{u}_n}{\partial t} + \mathbf{u}_n \cdot \nabla \mathbf{u}_n + f\mathbf{k} \times \mathbf{u}_n = -\frac{\nabla p_n}{\rho_1} + \frac{\tau}{\rho_1} + \text{Friction}, \quad \text{and} \tag{1}$$

$$\frac{\partial h_n}{\partial t} + \nabla \cdot \mathbf{u}_n h_n = 0, \tag{2}$$

where subscript n is the layer number: 1 for the upper layer and 2 for the lower layer. The terms $\mathbf{u}_n$, h_n, p_n, and ρ_n are the velocity, thickness, pressure, and density of the nth layer. The τ is the wind stress, which is only applied to the upper layer. The pressure gradient for the upper layer is $\nabla p_1/\rho_1 = g\nabla\eta_1$, where η_1 is the elevation of the free surface, and g is the surface gravity (9.8 m s^{-2}). The pressure gradient for the lower layer is $\nabla p_2/\rho_1 = g\nabla\eta_1 + g'\nabla\eta_2$, where η_2 is the elevation of the interface and $g' = g(\rho_2 - \rho_1)/\rho_1$ is the reduced gravity (0.02 m s^{-2}). The interface is initially set to 400-m depth (Fig. 6b). These parameters are set close to those commonly used to study the North Pacific (e.g., Qiu et al. 2015). This model is capable of handling vanishing layer thickness and behaves as a one-layer model in areas where the bottom topography is shallower than the interface (~400 m) but as a two-layer model where the interface exists. The friction term is the sum of subgrid-scale eddy viscosity, parameterized in a Laplacian form with a coefficient K_H of 100 $m^2 s^{-2}$ and a no-slip boundary condition and quadratic bottom drag with a drag coefficient of 0.03. Bottom drag acts only on the layer that is in direct contact with the bottom topography. To avoid the Kelvin waves from recirculating in the open ocean, viscosity coefficient is enhanced to $1 \times 10^4 m^2 s^{-2}$ near the model's southern and eastern boundaries.

The model domain is 6000 and 4000 km in the zonal and meridional directions, respectively, with a spatial resolution of 8.3 km (Fig. 6a). The β-plane approximation is used with the Coriolis parameter f at $1 \times 10^{-4} m s^{-1}$ at the center of the domain and β at $2 \times 10^{-11} s^{-1}$. There are two 4000-m-deep basins; the smaller one in the west represents the Japan Sea, and the larger one in the east represents the North Pacific (Fig. 6a). These basins are connected by two straits, which represent the Soya and Tsushima Straits. Both straits are 100 m deep and 40 km wide for simplicity, and continental shelves exist around the straits. These continental shelves are separated, similar to that around the Soya and Tsushima Straits. A third strait that represents the Tsugaru Strait will be added between the two straits in experiments to be presented later in section 4.

The model is initially at rest and is forced by an idealized wind stress field with a sinusoidal annual cycle and zero annual mean (Fig. 6a):

$$\tau = (\tau_N + \tau_E)\sin\left[\frac{2\pi(t-60)}{360}\right], \qquad (3)$$

where t is in days. One year is set to 360 days. The term τ_N represents the northerly winds in the Okhotsk Sea:

$$\tau_N = -0.2\exp\left(\frac{833.3-x}{416.7}\right)\left[1.0+\tanh\left(\frac{y-2917}{166.7}\right)\right],$$

where x and y are the zonal and meridional distances, respectively, from the lower-left corner in kilometers. The term τ_E represents the polar easterlies located around 60°N, along the northern boundary of the model domain:

$$\tau_E = -0.2\exp\left(\frac{y-4000}{416.7}\right)\exp\left(\frac{833.3-x}{416.7}\right).$$

The subtropical winds in the open ocean can be added but since we find its impact on the Throughflow negligible, as found in RTOPO (Fig. 4), we will not prescribe them here.

TABLE 1. Descriptions of the numerical experiments with two straits. Those with "—" are the same as CTRL.

	Surface gravity ($m^2 s^{-1}$)	Sill depth (m)	Basin bathymetry
CTRL	9.8	100	Idealized
WEAKG	0.098	—	—
DEEP	—	1000	—
SHELF-O	—	—	Shelf along the open ocean
SHELF-M	—	—	Shelf along the marginal sea

We will refer to the model experiment based on the setup above as CTRL. The model is integrated for 8 yr, which roughly corresponds to the time scale of baroclinic Rossby waves to cross the basin. We will examine the last 2 yr of this model run. The model setup for CTRL is set similar to RTOPO, and the main differences are the realistic winds and domain size. Since RTOPO is zonally longer than CTRL, the model is integrated for 16 yr. Biharmonic viscosity, with a coefficient of $2 \times 10^{10} m^4 s^{-1}$ and a slip boundary condition, is also used in RTOPO for numerical stability. All other setups are identical.

b. *Sensitivity experiments*

To better understand the dynamics of the Throughflow, some of the model components are modified from CTRL (Table 1). We will give brief descriptions here and provide the details later where the sensitivity results are presented.

The impact of barotropic adjustment is tested in WEAKG and DEEP. WEAKG has the surface gravity reduced by two orders of magnitude (0.098 $m^2 s^{-1}$). DEEP has the depth of the straits set deeper to 1000 m, which allows the isopycnal interfaces in the Japan Sea and the North Pacific to connect. The impact of the continental shelves is tested from SHELF-O and SHELF-M. SHELF-O has the continental shelves at the Soya and Tsushima Straits connected along the east coast of Japan. SHELF-M has the continental shelves connected along the coastlines of the Japan Sea. The impact of having three straits is tested from THREE, N-LONG, and S-LONG (Table 2). THREE has a third strait, which mimics the Tsugaru Strait, located between the two straits. N-LONG has a longer northern island, and S-LONG has a longer southern island.

3. Basinwide adjustment within the Japan Sea

The Throughflow simulated in CTRL shows the transports at the Tsushima and Soya Straits with an annual

TABLE 2. Descriptions of the numerical experiments with three straits.

	Winds	Basin bathymetry
THREE	Eq. (1)	Three straits
N-LONG	Eq. (1)	Longer northern island
S-LONG	Eq. (1)	Longer southern island
RTOPO	ERA-Interim monthly climatology	ETOPO1

cycle of about 0.3 Sv that changes synchronously (Fig. 7a). It captures the basic characteristics of the Throughflow observed at the two straits. The SSH also changes uniformly across the Japan Sea, a feature recognized in RTOPO (Fig. 5). The SSH during winter is positive (Fig. 7b), while that during summer is negative. Since the model conserves mass, the SSH in the open ocean will have an opposite sign on the spatial average but weaker signal because the spatial domain is much larger. The mass balance is roughly achieved by the flows through the straits, as expected for time scales longer than the subinertial period (Lyu and Kim 2005). The change of SSH is also not due to buoyancy forcing since the model is forced only by wind stress.

a. *Flow field simulated in CTRL*

CTRL shows that the wind along the northern and western coastlines of the open ocean is capable of driving the annual cycle of the Throughflow at the straits. Baroclinic Kelvin waves that are forced by the seasonal on/offshore Ekman transport at the northern/western boundaries are the main driver of this annual cycle. Minimum transport occurs in winter when the winds drive the onshore Ekman transport and vice versa, successfully explaining the observed annual cycle (Fig. 2). In absence of winds along the coast, such annual cycle is absent. We find the barotropic waves in the open ocean to play only a minor role on the annual cycle. When the model is simulated in absence of a layer interface (=only the upper layer) in the open ocean, the exchange flow is reduced by an order (not shown). The baroclinic component likely plays a more significant role because they create larger perturbations of the SSH along the coastlines of the open ocean, inducing larger seasonal changes of the SSH at the strait. This importance of baroclinicity is qualitatively consistent with the findings of Tsujino et al. (2008), in which a weak exchange flow is simulated in a GCM with no stratification. However, we further find the baroclinicity in the Japan Sea to play a minor role. When the model is simulated in absence of the layer interface in the Japan Sea, we find the magnitude of the annual cycle at the strait unchanged (not shown), suggesting the importance of barotropic dynamics there. A snapshot of the SSH and the interface in CTRL indeed shows such contrast in dynamics for the two basins (Fig. 7b). The perturbations are trapped near the coastlines in the open ocean but uniform in the Japan Sea.

The transformation of baroclinic to barotropic dynamics across the strait can be explained from how waves in the open ocean enter the Japan Sea (Fig. 8). The winds in the open ocean first excite baroclinic Kelvin waves, which propagate and encounter the continental shelf break near the Soya Strait. This excites the barotropic Kelvin waves at the shelf because only barotropic waves can exist there. Since the deformation radius of this wave is on the order of a few hundred kilometers, its signal not only affects the sea level above the continental shelf but also beyond the shelf break inside the Japan Sea. The surface gravity wave is thus excited in the Japan Sea and changes the sea level at the Tsushima Strait. Geostrophic adjustment then occurs and affects the Throughflow. With the surface gravity waves crossing the Japan Sea in a matter of a few hours, changes in the SSH occur uniformly, and the Throughflow at the Tsushima Strait should change simultaneously. This explains why the Throughflow at the two straits change synchronously in CTRL.

CTRL suggests that the annual cycle of the Throughflow occurs through the barotropic adjustment of the Japan Sea. This mechanism is similar to what is proposed by Kim and Fukumori (2008), who find barotropic adjustment to control the nonseasonal variability of the in/outflows in the Japan Sea based on satellite altimetry. Our model results indicate that such a mechanism is also applicable for the annual cycle. Our results are also in line with the study of Ohshima (1994), where the surface gravity waves are shown to be responsible as the first stage of adjustment at the straits. The importance of barotropic adjustment likely arises because the spatial scale of the Japan Sea is roughly within the barotropic deformation radius $\sqrt{(gH)}/f$, which is about 1200 km for a 1500-m-deep basin. Barotropic signals therefore occur uniformly across the sea. Furthermore, the continental shelves are narrower than the barotropic deformation radius there (about 400 km), so the perturbation at the strait can reach the deeper part of the Japan Sea almost simultaneously.

b. *The role of barotropic waves*

The importance of barotropic waves on the annual cycle of the Throughflow is tested from two sensitivity experiments. The first experiment reduces the surface gravity by two orders of magnitude but keeps the reduced gravity the same so that the internal Kelvin wave speed is unchanged (WEAKG). We find the annual

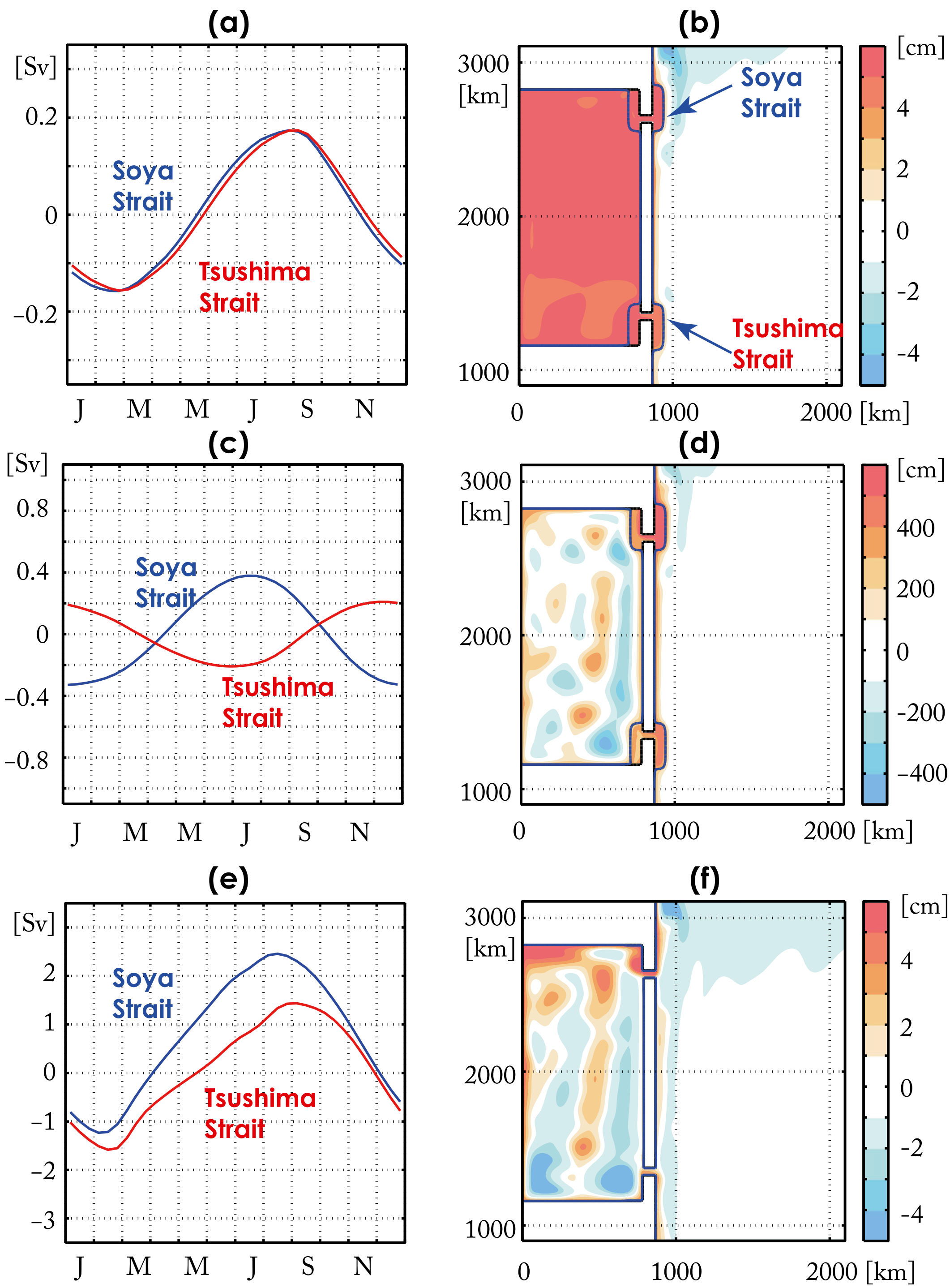

FIG. 7. (a) The 10-day-averaged transports at the Soya and Tsushima Straits from CTRL. Positive values are toward the Japan Sea for the Tsushima Strait but toward the North Pacific for the Soya Strait, reflecting the direction of the annual-mean Throughflow. (b) The monthly mean SSH in January from CTRL. The blue lines show the 400-m depth contours. (c),(d) As in (a) and (b), but for WEAKG. (e),(f) As in (a) and (b), but for DEEP. Note the difference in the y axis for the figures on the left and the color range for the figures on the right.

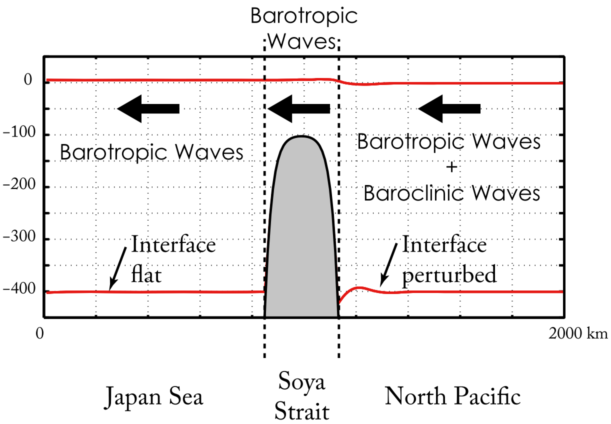

FIG. 8. A schematic of how waves propagate from the North Pacific to the Japan Sea across the Soya Strait. The SSH and interface simulated in CTRL for January are drawn in red. SSH is magnified 100 times for clarity. Perturbations are coastally trapped near the shelf of the North Pacific but are uniform in the Japan Sea.

cycle in WEAKG to enhance to 0.8 Sv, but the Throughflow at the Soya and Tsushima Straits no longer changes synchronously (Fig. 7c). They are now out of phase. If barotropic waves were insignificant in CTRL, the Throughflow should have shown a similar annual cycle in WEAKG as that of CTRL. The Kelvin waves that propagate along the coasts of the Japan Sea cyclonically are observed, but they take more time to reach from the Soya Strait to the Tsugaru Strait compared to that propagating along the east coast of Japan (Fig. 7d). As a result, the annual cycle of the Throughflow is mainly induced by the waves propagating along the east coast of Japan, not by the waves propagating within the Japan Sea. WEAKG reveals that the barotropic waves are an essential component of the dynamics that make the annual cycle of the Throughflow change synchronously at all straits.

The second experiment examines the role of the shallow straits on the transfer of baroclinic to barotropic waves between the Japan Sea and the North Pacific by deepening the straits from 100 to 1000 m (DEEP). With the straits deeper than the interface (~400 m), baroclinic Kelvin waves can penetrate the straits without transforming to barotropic Kelvin waves. The internal deformation radius is about 20 km, so the baroclinic waves are also capable of penetrating the straits. As expected, we find the Throughflow in DEEP to enhance significantly by one order of magnitude (4 Sv) (Fig. 7e). Moreover, the SSH signal in the Japan Sea is coastally trapped, which is continuous from the open ocean to the Japan Sea (Fig. 7f) rather than uniform as found in CTRL. The slight delay of the Throughflow at the Tsushima Strait likely reflects the impact of the baroclinic Kelvin wave propagating along the Japan Sea since it takes roughly 10–15 days to propagate from the Soya Strait to the Tsushima Strait along the coastline.

c. *The role of continental slopes*

The importance of bottom topography between the two straits is tested from two sensitivity experiments. Bottom topography can significantly modify how the waves propagate, and, since the continental shelves at the Soya and Tsushima Straits are separated in CTRL, we will connect them in two ways.

The first experiment, SHELF-O, connects the continental shelves along the east coast of Japan (Fig. 9a). SHELF-O tests our hypothesis that the annual cycle is strongly governed by the waves that propagate across the Japan Sea rather than that along the open ocean. With the continental shelves now connected along the east coast of Japan, the barotropic Kelvin waves that are excited near the Soya Strait can quickly propagate along this shelf and affect the SSH at the Tsushima Strait. Indeed, the annual cycle in SHELF-O show a much reduced magnitude in the annual cycle (Fig. 9b). Minimum transport is also observed in fall rather than winter. Unlike CTRL, the SSH show similar values across the straits (Fig. 9c), which explains why the reduction of the Throughflow occurs.

The second experiment, SHELF-M, connects the continental shelves along the coastlines of the Japan Sea (Fig. 9d). With such shelves, part of the barotropic Kelvin waves that are excited near the Soya Strait can propagate along the shelves without transferring to basin-scale barotropic waves. We find the annual cycle in SHELF-M to be about 0.4 Sv (Fig. 9e), which is a slight increase from CTRL, but the basic features remain similar to CTRL. The SSH also shows the signal of the shelf waves to be weak and the majority of the SSH change uniformly across the basin (Fig. 9f). This is likely because the shelves are narrower than the spatial scale of the barotropic Kelvin waves. The shelf waves also reach the Tsushima Strait within a matter of a few hours, similar to the basin-scale waves, so the presence of the shelf wave has a minor impact on the annual cycle when examined on the monthly time scale.

4. The annual cycle at the Tsugaru Strait

The dynamics of the Throughflow at the Tsugaru Strait is examined by adding a third strait (THREE). This strait is 40 km wide, 100 m deep, and has a continental shelf just like other straits. It is also located closer to the Soya Strait (Fig. 10b). We find THREE to simulate an annual cycle of the Throughflow at the Tsugaru

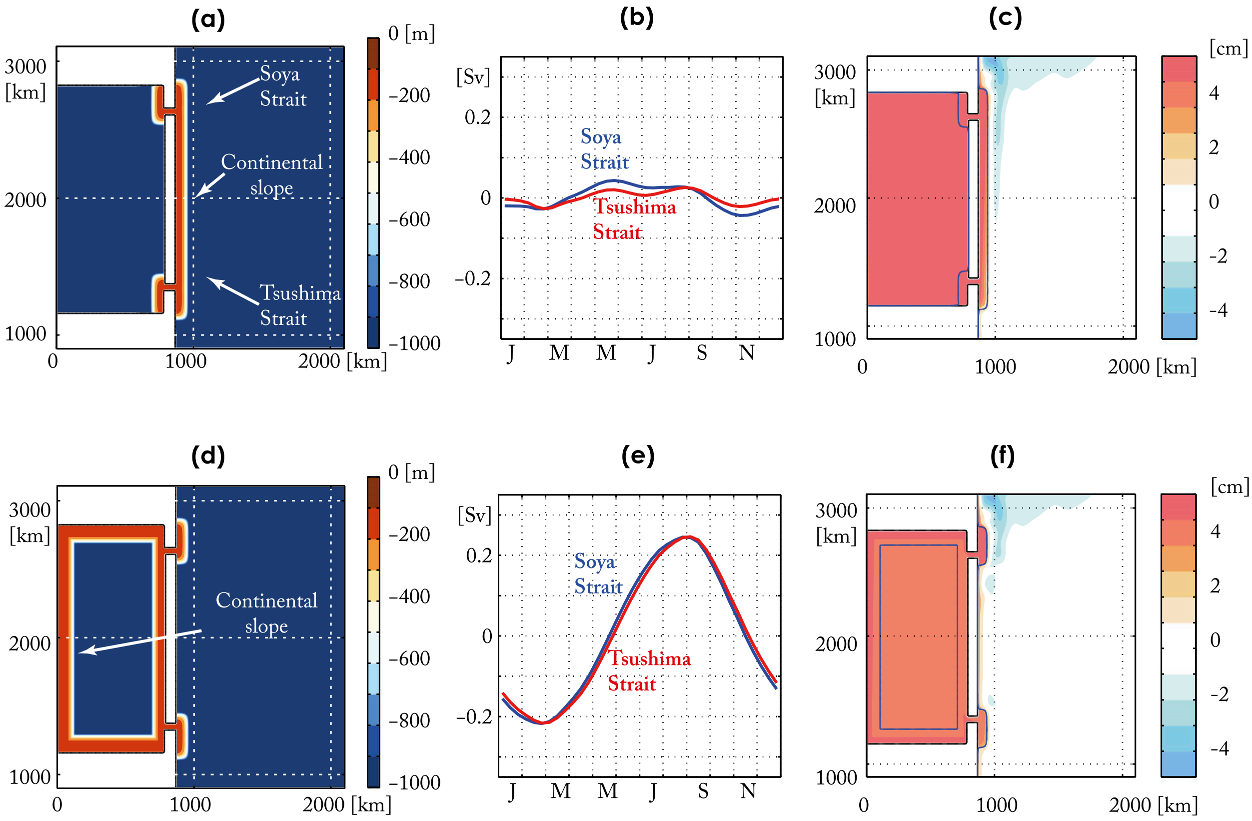

FIG. 9. (a) Bottom topography used in SHELF-O. (b) Monthly mean transport at the Tsushima and Soya Straits and (c) monthly mean SSH in January from SHELF-M. (d),(e),(f) As in (a), (b), and (c), but for SHELF-O.

Strait with a significantly weaker magnitude (2×10^{-2} Sv) (Fig. 10a). The Throughflow at the Soya and Tsushima Straits as well as the SSH within the Japan Sea remain similar to CTRL (Fig. 7a).

a. Frictional balance around an island

How is the Throughflow at the Tsugaru Strait controlled? We find an integral constraint, based on frictional stress exerted around an island, useful in understanding the mechanism. This equation can be derived from integrating the momentum equation around an island:

$$0 = \oint_C (K_H \nabla \cdot \nabla u)\, dl, \tag{4}$$

where C is the line integral around an island [Fig. 11a; see Kida and Qiu (2013) or Yang (2007) for derivation]. What Eq. (4) shows is that frictional stresses exerted around an island must integrate to zero, and Yang (2007) refers to this equation as the around-island integral constraint. Equation (4) appears similar to the classic Kelvin's circulation theorem where an inviscid and unforced circulation is assumed, but here we consider the presence of viscosity and a no-slip boundary condition. Using Eq. (4), Kida and Qiu (2013) assumed a frictional balance between the stresses exerted by a Throughflow and that by the WBC and showed that the magnitude of the Throughflow transport U scales as

$$U = \frac{Q}{1 + 16\alpha\gamma^{-3}}, \tag{5}$$

where α is the ratio of the zonal and meridional lengths of an island L_x/L_y; γ is the ratio of the width of the strait compared to the Munk boundary layer width l/δ_M; and Q is the transport of the WBC. Equation (5) shows that a WBC from the north can drive a Throughflow in the marginal sea in a cyclonic sense with its magnitude controlled by two nondimensional parameters α and γ.

Since Eq. (5) is for two straits, we need to extend it for three straits to understand the Japan Sea. By applying Eq. (4) for two islands and by assuming the same frictional balance between the flow through the straits and the WBC as in Kida and Qiu (2013), we derive two equations,

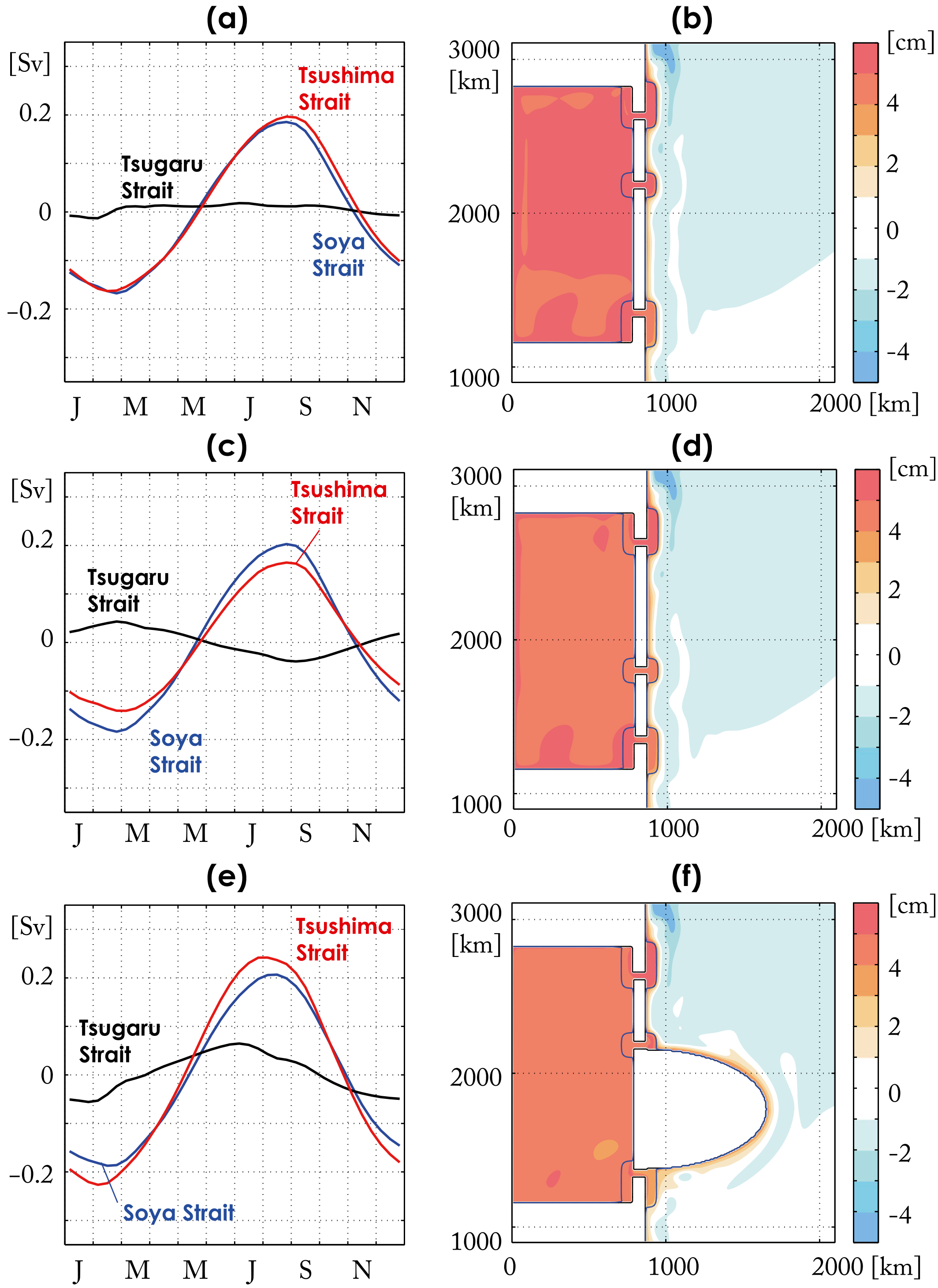

FIG. 10. (a) The annual cycle of the Throughflow from THREE. Red, black, and blue lines are the transports through the Tsushima, Tsugaru, and Soya Straits, respectively. Positive values are toward the Japan Sea for the Tsushima Strait but toward the North Pacific for the Soya and Tsugaru Straits, reflecting the direction of the annual-mean Throughflow. (b) Monthly averaged SSH in January from THREE. The blue lines show the 400-m depth contours. (c),(d) As in (a) and (b), but for N-LONG. (e),(f) As in (a) and (b), but for S-LONG.

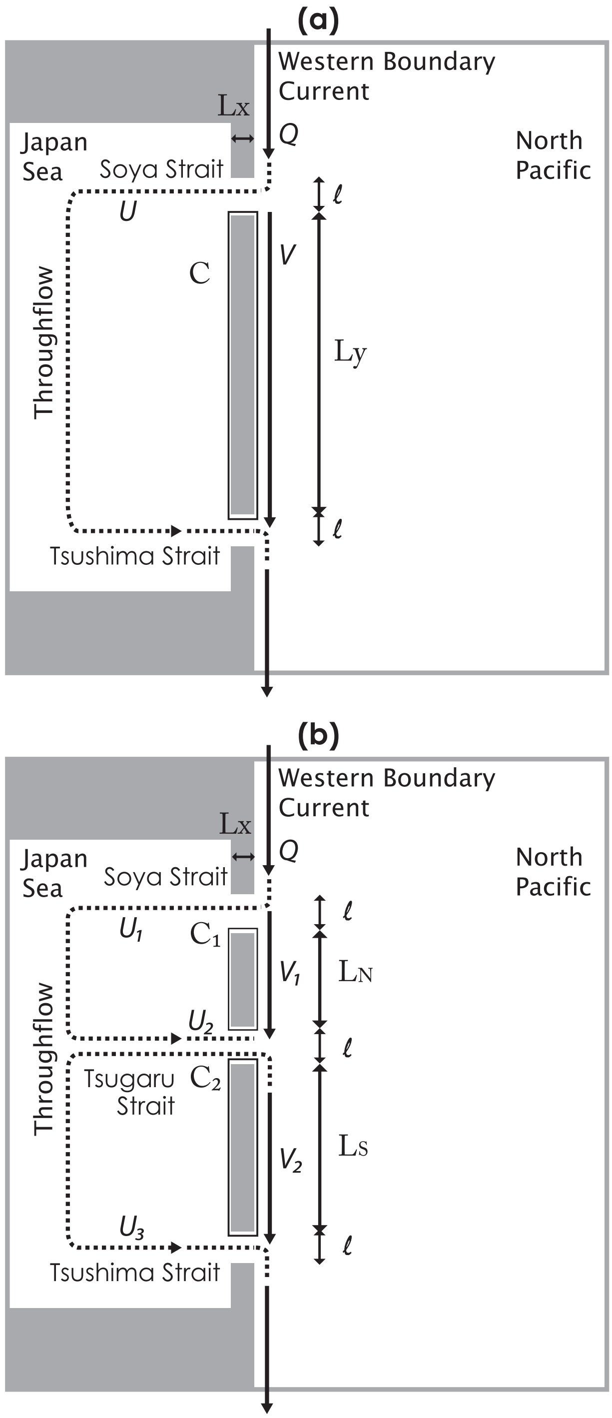

FIG. 11. A schematic of the Throughflow when there are (a) two straits and (b) three straits. The WBC (Q) flows from the northwest coast of the North Pacific and drives the Throughflow in the Japan Sea (U). The C is the line integral around an island. Notice that the flow through the strait in the middle is a sum of two Throughflows driven in opposite directions. The parameters used in Eqs. (4)–(8) are also shown.

$$K_H \frac{U_1/(h\delta_1)}{\delta_1^2} L_x - K_H \frac{(-U_2)/(h\delta_2)}{\delta_2^2} L_x = K_H \frac{V_1/(H\delta_M)}{\delta_M^2} L_N, \tag{6}$$

and

$$-K_H \frac{U_2/(h\delta_2)}{\delta_2^2} L_x - K_H \frac{(-U_3)/(h\delta_3)}{\delta_3^2} L_x = K_H \frac{V_2/(H\delta_M)}{\delta_M^2} L_S, \tag{7}$$

for the northern and southern islands, respectively (Fig. 11b). V is the magnitude of the WBC transport along the eastern coast of an island. The frictional stresses are scaled as $K_H(\Delta u/\delta^2) \times$ LengthScale, where δ is the frictional boundary layer scale. The terms on the LHS of Eqs. (6) and (7) are the frictional stresses exerted by the Throughflow at the straits, and the term on the RHS is that exerted by the WBC. The term h is the thickness of the Throughflow at the strait (~depth of the strait); H is the thickness of the WBC (~depth of the interface). Positive transport at the Tsugaru Strait is defined toward the North Pacific. Subscripts 1, 2, and 3 are for the Soya, Tsugaru, and Tsushima Straits, respectively. Subscripts N and S are for the northern and southern islands, respectively. When assuming that the frictional boundary layer at the three straits are half the width of the straits for simplicity, Eqs. (6) and (7) can be combined with the mass balance equations $U_1 + V_1 = Q$, $U_3 + V_2 = Q$ and $U_1 - U_2 = U_3$ to derive a scaling solution for U_2:

$$U_2 = \frac{(F_N - F_S)Q}{1 + 8F_N\alpha_1\gamma^{-3}\lambda^{-1} + 8F_S\alpha_2\gamma^{-3}\lambda^{-1}}, \tag{8}$$

where $F_N = (1 + 8\alpha_1\gamma^{-3}\lambda^{-1})^{-1}$ and $F_S = (1 + 8\alpha_2\gamma^{-3}\lambda^{-1})^{-1}$. The terms F_N and F_S represent the impact of the frictional stresses around the northern and southern islands, respectively. The equation $\lambda = h/H$ is the ratio of the strait depth compared to the interface depth. It is worth pointing out that the use of the mass balance equation is appropriate here based on the assumption that the barotropic waves enable the Throughflow at the three straits to balance mass on the monthly time scale.

b. *Sensitivity to the Throughflow*

Equation (8) shows that the flow through the Tsugaru Strait is determined from a competition of frictional stresses exerted around the two islands (Fig. 11b). For the Tsugaru Strait, the flows induced around the northern and southern islands are in opposite directions. It is this cancellation that makes the Throughflow weaker than those at the Soya and Tsushima Straits.

Equation (8) also shows that the direction of U_2 depends on the sign of $F_N - F_S$, which is determined from

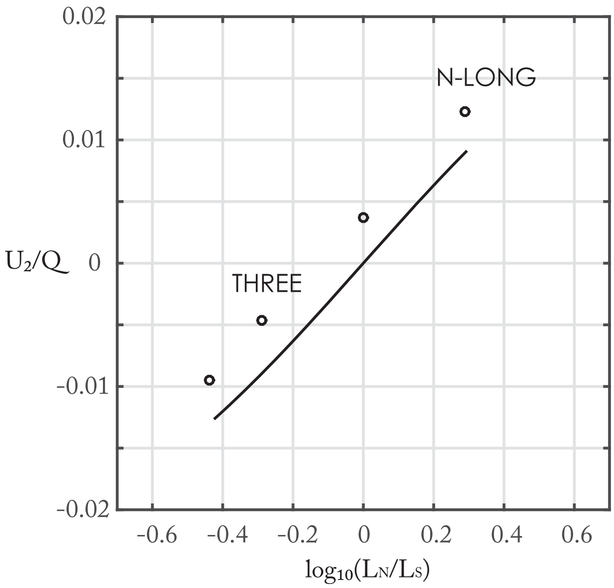

FIG. 12. The sensitivity of the Throughflow at the Tsugaru Strait U_2 to L_N/L_S, the ratio of meridional length scale of the northern and southern islands. Circles are model results and the solid line is from Eq. (8). The U_2 is nondimensionalized by Q, the transport of the WBC estimated upstream of Soya Strait.

the difference of α_1 and α_2 and thus the meridional length scale of the two islands. When the southern island is longer, $F_N - F_S$ is negative and so the flow would be in the same direction as that at the Soya Strait. This is what is observed in THREE. Indeed, when the southern island is even longer (S-LONG), we observe an enhancement of the annual cycle (Figs. 10e,f). When the northern island is longer than the southern island instead, we find the flow going toward the opposite direction (N-LONG; Figs. 10c,d). Model experiments support that the flow through the Tsugaru Strait is sensitive to the length scales of the islands and that Eq. (8) explains this behavior well (Fig. 12). The model appears to show a stronger role of the frictional stresses around the northern island, which tends to drive a positive transport at the Tsugaru Strait compared to that suggested from Eq. (8). Note that the frictional boundary layer within the strait is estimated as 10 km based on the model results in Fig. 12, rather than half the width of the straits (20 km) since the presence of inertia acts to narrow this length scale especially at the northern strait (Kida and Qiu 2013).

The annual cycle at the Tsugaru Strait is weak in THREE (Figs. 9a,b) but quite robust in RTOPO (Fig. 3b). Changes in the steepness of the slope may have affected the magnitude of the frictional stress. We suspect part of the difference also comes from the meridional length scale of the islands used in THREE. While the latitudinal locations of the straits roughly represent those of the Soya, Tsugaru, and Tsushima Straits, the actual distance between the straits are different. For example, the islands south of the Tsugaru Strait actually bend toward the west, and so the distance between the Tsugaru and Tsushima Straits is about 1500 km or more (Fig. 1). This is much longer than the distance between the Tsugaru and Soya Straits used in THREE and more similar to S-LONG, where a significant enhancement of the annual cycle is observed at the Tsugaru Strait (Figs. 10e,f).

5. Summary and concluding remarks

The dynamics responsible for the annual cycle of the Japan Sea Throughflow were examined using a two-layer isopycnal model. We raised two specific questions at the beginning and here we summarize the results.

a. *What is the primary forcing agent of the annual cycle?*

The subpolar winds along the coastlines are likely playing the leading role and the basic mechanism is as follows:

1) The subpolar winds induce baroclinic Kelvin waves along the coastlines of the subpolar gyre.
2) The SSH at the continental shelf of the Soya Strait changes and modifies the Throughflow transport.
3) Barotropic adjustment occurs in the Japan Sea and modifies the Throughflow transports at the Tsushima and Tsugaru Straits.

The importance of the subpolar winds on the mean and annual cycle of the Throughflow transport has been emphasized in previous studies (e.g., Tsujino et al. 2008; Yang et al. 2013), but those studies focused on the adjustments in the open ocean. Here, we emphasize the role of barotropic adjustment inside the Japan Sea rather than the baroclinic waves. The SSH anomaly found in Tsujino et al.'s (2008) GCM simulations (their Figs. 4c and 4d) appears to support the uniform SSH changes. The role of westerlies in the subtropics is secondary, and most of its impact likely comes from the monsoonal winds around Japan rather than the winds in the open ocean. The monsoonal winds along the east coast of Japan can force baroclinic Kelvin waves that affect the Throughflow transport from the Tsushima Strait, similar to the mechanism presented above. However, the significance of this pathway depends on the magnitude of the winds near the coastline of Japan and thus may be sensitive to the wind product used. Baroclinic upper-ocean circulation within the Japan Sea may also affect the SSH at the straits and the

Throughflow, although we find this process to play a minor role, at least for the annual cycle.

Our study suggests that the mechanism behind the annual cycle of the Throughflow is unlikely to be that based on the use of the extended island rule (Seung et al. 2012) because this idea assumes the wind stress curl in the open ocean as the forcing agent. Similarly, we consider the open-ocean forcing mechanism of Ma et al. (2012) to be better interpreted as the role of subpolar winds and the waves forced along the northern boundary rather than the subtropical winds in the ocean interior. Such a distinction could not be made because their model experiments did not separate the role of subtropical versus subpolar winds. This is not to say that the frictional stresses exerted by the Kuroshio and the Tsushima Warm Current do not balance. In fact, we make roughly the same assumption as in Ma et al. (2012) when deriving Eq. (8).

b. Why is the annual cycle at the Tsugaru Strait smaller than the other straits?

The magnitude of the Throughflow at the Tsugaru Strait is weak because it is located between the northern (Hokkaido) and southern (Honshu) islands. The flow there needs to satisfy the frictional balance around both islands, which has a tendency to force a flow in opposite directions. Frictional balance further shows that the direction of the Throughflow at the Tsugaru Strait depends on the length scales of the two islands [Eq. (8)]. The phase of the annual cycle at the Tsugaru Strait is likely similar to that of Soya Strait because the southern island is longer than the northern counterpart is.

The two-layer model used in this study obviously has its limitations. The impact of stratification cannot be fully resolved, such as that within the thermocline. While the time scale of dynamical adjustment tends to be longer for higher-order baroclinic effects, the subtropical gyre is more stratified than the subpolar gyre and so the role of subtropical winds on the Throughflow may be more sensitive to this effect. Nonetheless, the two-layer model was successful at illuminating the role of barotropic adjustment in the Japan Sea. The barotropic response within marginal seas has been assumed (Lyu and Kim 2005) or suggested in the past for a relatively short time-scale variability (Fukumori et al. 2007; Kim and Fukumori 2008), but it is a feature that is often overlooked and the process needs to be further explored from observational data as well. Do barotropic dynamics also matter for the interannual and decadal variability of the Japan Sea Throughflow? Where is its primary forcing region? Gordon and Giulivi (2004) relate the Tsushima Current transport to the strength of the Kuroshio south of Japan on the decadal time scale. The Throughflow may be affected by the changes in the Kuroshio transport, which is induced by climate variability occurring in lower latitudes, if the Kuroshio can significantly change the sea surface height along the southern coast of Japan. We consider such questions the next step of our investigations.

Acknowledgments. The authors thank two anonymous reviewers for many useful comments. S. Kida is supported by KAKENHI (22106002). B. Qiu is supported by NASA (NNX13AE15G). J. Yang is supported by the U.S. National Science Foundation. X. Lin is supported by the Natural Science Foundation of China (41222037 and U1406401), China's National Basic Research Priorities Programme (2013CB956202), and the Global Air-Sea Interaction Project (GASI-03-01-01-02).

REFERENCES

Andres, M., Y.-O. Kwon, and J. Yang, 2011: Observations of the Kuroshio's barotropic and baroclinic responses to basin-wide wind forcing. *J. Geophys. Res.*, **116**, C04011, doi:10.1029/2010JC006863.

Cho, Y.-K., G.-H. Seo, B.-J. Choi, S. Kim, Y.-G. Kim, Y.-H. Youn, and E. P. Dever, 2009: Connectivity among straits of the northwest Pacific marginal seas. *J. Geophys. Res.*, **114**, C06018, doi:10.1029/2008JC005218.

——, ——, C.-S. Kim, B.-J. Choi, and D. C. Shaha, 2013: Role of wind stress in causing maximum transport through the Korea Strait in autumn. *J. Mar. Syst.*, **115–116**, 33–39, doi:10.1016/j.jmarsys.2013.02.002.

Dee, D. P., and Coauthors, 2011: The ERA-Interim reanalysis: Configuration and performance of the data assimilation system. *Quart. J. Roy. Meteor. Soc.*, **137**, 553–597, doi:10.1002/qj.828.

Fukamachi, Y., I. Tanaka, K. I. Ohshima, N. Ebuchi, G. Mizuta, H. Yoshida, S. Takayanagi, and M. Wakatsuchi, 2008: Volume transport of the Soya Warm Current revealed by bottom-mounted ADCP and ocean-radar measurement. *J. Oceanogr.*, **64**, 385–392, doi:10.1007/s10872-008-0031-3.

Fukudome, K., J.-H. Yoon, A. Ostrovskii, T. Takikawa, and I.-S. Han, 2010: Seasonal volume transport variation in the Tsushima Warm Current through the Tsushima Straits from 10 years of ADCP observations. *J. Oceanogr.*, **66**, 539–551, doi:10.1007/s10872-010-0045-5.

Fukumori, I., D. Menemenlis, and T. Lee, 2007: A near-uniform basinwide sea level fluctuations of the Mediterranean Sea. *J. Phys. Oceanogr.*, **37**, 338–358, doi:10.1175/JPO3016.1.

Godfrey, J. S., 1989: A Sverdrup model of the depth-integrated flow for the World Ocean allowing for island circulations. *Geophys. Astrophys. Fluid Dyn.*, **45**, 89–112, doi:10.1080/03091928908208894.

Gordon, A. L., and C. F. Giulivi, 2004: Pacific decadal oscillation and sea level in the Japan/East Sea. *Deep-Sea Res. I*, **51**, 653–663, doi:10.1016/j.dsr.2004.02.005.

Guo, X., Y. Miyazawa, and T. Yamagata, 2006: The Kuroshio onshore intrusion along the shelf break of the East China Sea: The origin of the Tsushima Warm Current. *J. Phys. Oceanogr.*, **36**, 2205–2231, doi:10.1175/JPO2976.1.

Hallberg, R., 1997: Stable split time steeping schemes for large-scale ocean modeling. *J. Comput. Phys.*, **135**, 54–65, doi:10.1006/jcph.1997.5734.

Hirose, N., and K. I. Fukudome, 2006: Monitoring the Tsushima Warm Current improves seasonal prediction of the regional snowfall. *SOLA*, **2**, 61–63, doi:10.2151/sola.2006-016.

Imawaki, S., H. Uchida, H. Ichikawa, M. Fukasawa, and S. Umatani, 2001: Satellite altimeter monitoring the Kuroshio transport south of Japan. *Geophys. Res. Lett.*, **28**, 17–20, doi:10.1029/2000GL011796.

Isobe, A., 2008: Recent advances in ocean-circulation research on the Yellow Sea and East China Sea shelves. *J. Oceanogr.*, **64**, 569–584, doi:10.1007/s10872-008-0048-7.

——, and S. Imawaki, 2002: Annual variation of the Kuroshio transport in a two-layer numerical model with a ridge. *J. Phys. Oceanogr.*, **32**, 994–1009, doi:10.1175/1520-0485(2002)032<0994:AVOTKT>2.0.CO;2.

——, M. Ando, T. Watanabe, T. Senjyu, S. Sugihara, and A. Manda, 2002: Freshwater and temperature transports through the Tsushima-Korea Straits. *J. Geophys. Res.*, **107**, 3065, doi:10.1029/2000JC000702.

Kida, S., and B. Qiu, 2013: An exchange flow between the Okhotsk Sea and the North Pacific driven by the East Kamchatka Current. *J. Geophys. Res. Oceans*, **118**, 6747–6758, doi:10.1002/2013JC009464.

Kim, S.-B., and I. Fukumori, 2008: A near uniform basin-wide sea level fluctuation over the Japan/East Sea: A semienclosed sea with multiple straits. *J. Geophys. Res.*, **113**, C06031, doi:10.1029/2007JC004409.

Lyu, S. J., and K. Kim, 2003: Absolute transport from the sea level difference across the Korea Strait. *Geophys. Res. Lett.*, **30**, 1285, doi:10.1029/2002GL016233.

——, and ——, 2005: Subinertial to interannual transport variations in the Korea Strait and their possible mechanisms. *J. Geophys. Res.*, **110**, C12016, doi:10.1029/2004JC002651.

Ma, C., D. Wu, X. Lin, J. Yang, and X. Ju, 2012: On the mechanism of seasonal variation of the Tsushima Warm Current. *Cont. Shelf Res.*, **48**, 1–7, doi:10.1016/j.csr.2012.08.013.

Minato, S., and R. Kimura, 1980: Volume transport of the western boundary current penetrating into a marginal sea. *J. Oceanogr. Soc. Japan*, **36**, 185–195, doi:10.1007/BF02070331.

Moon, J. H., N. Hirose, J. H. Yoon, and I. C. Pang, 2009: Effect of the along-strait wind on the volume transport through the Tsushima/Korea Strait in September. *J. Oceanogr.*, **65**, 17–29, doi:10.1007/s10872-009-0002-3.

Nakanowatari, T., and K. I. Ohshima, 2014: Coherent sea level variation in and around the Sea of Okhotsk. *Prog. Oceanogr.*, **126**, 58–70, doi:10.1016/j.pocean.2014.05.009.

Nishida, Y., I. Kanomata, I. Tanaka, S. Sato, S. Takahashi, and H. Matsubara, 2003: Seasonal and interannual variations of the volume transport through the Tsugaru Strait (in Japanese with English abstract). *Umi no Kenkyu*, **12**, 487–499.

Ohshima, K. I., 1994: The flow system in the Japan Sea caused by a sea level difference through shallow straits. *J. Geophys. Res.*, **99**, 9925–9940, doi:10.1029/94JC00170.

——, and D. Simizu, 2008: Particle tracking experiments on a model of the Okhotsk Sea: Toward oil spill simulation. *J. Oceanogr.*, **64**, 103–114, doi:10.1007/s10872-008-0008-2.

Onishi, M., and K. Ohtani, 1997: Volume transport of the Tsushima Warm Current, west of Tsugaru Strait bifurcation area. *J. Oceanogr.*, **53**, 27–34, doi:10.1007/BF02700746.

Qiu, B., S. Chen, L. Wu, and S. Kida, 2015: Wind- versus eddy-forced regional sea level trend and variability in the North Pacific Ocean. *J. Climate*, **28**, 1561–1577, doi:10.1175/JCLI-D-14-00479.1.

Seo, H., Y.-O. Kwon, and J.-J. Park, 2014: On the effect of the East/Japan Sea SST variability on the North Pacific atmospheric circulation in a regional climate model. *J. Geophys. Res. Atmos.*, **119**, 418–444, doi:10.1002/2013JD020523.

Seung, Y.-H., 2003: Significance of shallow bottom friction in the dynamics of the Tsushima Current. *J. Oceanogr.*, **59**, 113–118, doi:10.1023/A:1022828825667.

——, S.-Y. Han, and E.-P. Lim, 2012: Seasonal variation of volume transport through the straits of the East/Japan Sea viewed from the island rule. *Ocean Polar Res.*, **34**, 403–411, doi:10.4217/OPR.2012.34.4.403.

Shikama, N., 1994: Current measurement in the Tsugaru Strait using bottom-mounted ADCPs (in Japanese). *Kaiyo Mon.*, **26**, 815–818.

Takikawa, T., and J.-H. Yoon, 2005: Volume transport through the Tsushima Straits estimated from sea level difference. *J. Oceanogr.*, **61**, 699–708, doi:10.1007/s10872-005-0077-4.

——, ——, and K.-D. Cho, 2005: The Tsushima Warm Current through Tsushima Straits estimated from ferryboat ADCP data. *J. Phys. Oceanogr.*, **35**, 1154–1168, doi:10.1175/JPO2742.1.

Talley, L. D., and Coauthors, 2006: Japan/East Sea water masses and their relation to the sea's circulation. *Oceanography*, **19**, 32–49, doi:10.5670/oceanog.2006.42.

Teague, W. J., G. A. Jacobs, H. T. Perkins, J. W. Book, K.-I. Chang, and M.-S. Suk, 2002: Low-frequency current observations in the Korea/Tsushima Strait. *J. Phys. Oceanogr.*, **32**, 1621–1641, doi:10.1175/1520-0485(2002)032<1621:LFCOIT>2.0.CO;2.

——, and Coauthors, 2006: Currents through the Korea/Tsushima Strait: A review of LINKS observations. *Oceanography*, **19**, 50–63, doi:10.5670/oceanog.2006.43.

Tsujino, H., H. Nakano, and T. Motoi, 2008: Mechanism of currents through the straits of the Japan Sea: Mean state and seasonal variation. *J. Oceanogr.*, **64**, 141–161, doi:10.1007/s10872-008-0011-7.

Yamamoto, M., and N. Hirose, 2011: Possible modification of atmospheric circulation over the northwestern Pacific induced by a small semi-enclosed ocean. *Geophys. Res. Lett.*, **38**, L03804, doi:10.1029/2010GL046214.

Yang, J., 2007: An oceanic current against the wind: How does Taiwan Island steer warm water into the East China Sea? *J. Phys. Oceanogr.*, **37**, 2563–2569, doi:10.1175/JPO3134.1.

——, X. Lin, and D. Wu, 2013: Wind-driven exchanges between two basins: Some topographic and latitudinal effects. *J. Geophys. Res. Oceans*, **118**, 4585–4599, doi:10.1002/jgrc.20333.